International Journal of Electrical and Electronics Research ISSN 2348-6988 (online)
Vol. 2, Issue 2, pp: (140-150), Month: April - June 2014, Available at: www.researchpublish.com

Boundary-Mode Operation of the Boost Converter for Thermoelectric Generator Maximum Power Tracking

Michael P. Theodoridis

Brunel University London, UK

Abstract: **Performance-favourable and noteworthy characteristics of the Boost converter are reported, when the latter operates in Maximum Power Tracking (MPT) mode, while fed from a fixed internal resistance power source specifically a Thermo Electric Generator (TEG). It is found that if the converter is controlled with Pulse Frequency Modulation (PFM), for a specific value of inductance, the inductor current inherently remains on the boundary of continuity for the whole control range, that is under all conditions, resulting in reduced switching losses. Furthermore, MPT is possible without the sampling of any current but only with the sampling of the converter input and output voltages. The above theoretical findings have been verified by an experimental prototype.**

Keywords: **Boost Converter, Maximum Power Tracking, Super capacitor, Energy storage.**

I. INTRODUCTION

A thermoelectric generator is capable of generating electricity by exploiting a temperature difference in a thermal system. This is a particularly useful arrangement in wasted heat recovery systems, such as those currently tested on combustion engine vehicles, where a TEG is used to exploit the temperature difference between the vehicle exhaust and the ambient air [1,2]. The produced electrical power can be high enough to negate the need for an electromechanical alternator, thereby enhancing the overall engine efficiency. Due to the low output voltage of TEG cells, a Boost converter is typically used to interface the cells to the electrical load, [3,4,5,6,7,8].

Because of the variation of the cell voltage, due to temperature variations, and the variations of the load resistance, an MPT control method is also typically employed [3,4,5,7] in order to extract maximum power under all conditions from the TEG cell. The MPT methods, similar to those used with photovoltaic cells, normally require one or more of the following: current sensing [5,9], fractional open or short circuits [3, 10], tuned Pertrube & Observe (PO) algorithms, Incremental Conductance (INC) algorithms [5,11].

Recent development in this field has been the employment of a Zero Current Switching (ZCS) technique in order to reduce the converter losses [12, 13], with a more recent one that works in conjunction with a fractional short-circuit MPT control method, [4]. In these systems, instead of Pulse Width Modulation (PWM), PFM is employed, where a constant ON time is used for the control of the converter power switch, while the switching frequency is varied in order to achieve MPT.

An alternative PFM-based, control method is proposed in this paper, with its relative merits and disadvantages, but mostly revealing noteworthy inherent properties of the Boost converter. These properties are as follows: a) while performing MPT, the Boost converter, if operated with PFM, and for a specific value of inductance, remains on the boundary between Continuous Inductor Current Mode (CICM) and Discontinuous Inductor Current Mode (DICM) for the whole MPT control range, and b) MPT can be achieved only with the sampling of the input and output voltages. These properties lead to the advantage of naturally achieving ZCS, resulting in reduced switching losses. Also, MPT can be implemented easily

and allows for variable output voltage. This means that a super capacitor may be used for energy storage at the output of the converter, Fig.1, with its varying voltage not affecting the MPT process, contrary to methods which require a fixed output voltage, i.e. a battery. This system forms a candidate for a heat recovery arrangement, where energy storage is required in order to reject the variations of the output of TEG cells, such as the variation of a vehicle's exhaust gas temperature at different operating regimes; for example idle and full throttle.

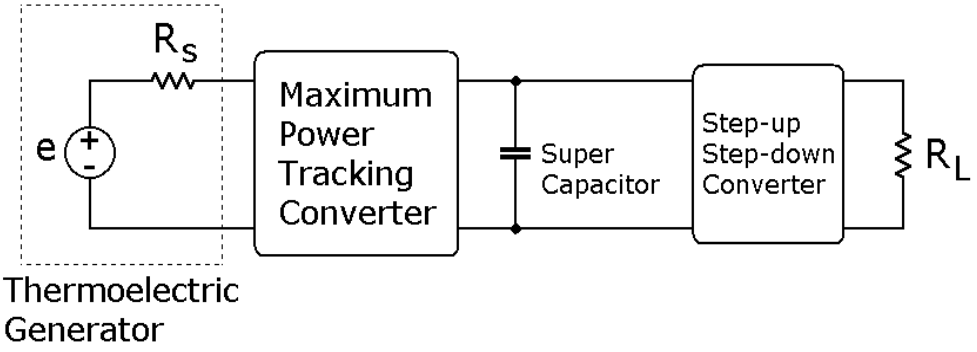

Fig. 1 *Block diagram of the system under investigation.*

In the following section a number of comparative analyses will be presented. First it will be shown why operating the converter in DICM, instead of CICM, allows for easier implementation of MPT. Then, further to that, it is shown that operating in DICM requires less control effort than in CICM. Finally, a comparative analysis between operating with PWM and PFM reveals the property of the proposed system to operate on the boundary between continuous and discontinuous inductor current, and a microprocessor-controlled experimental prototype verifies the above findings.

II. MAXIMUM POWER TRACKING ANALYSIS

A. Assumptions

For the analyses presented below, the thermoelectric generator is modelled as a voltage source, whose amplitude is a function of the temperature difference between its two surfaces, and an equivalent series resistance, Fig.1. It has been shown by measurements in [14] and [15] that this resistance is fairly constant and independent of the thermal energy applied to the TEG. In order to extract maximum power from the generator one needs to present it with a load of resistance equal to the equivalent internal series resistance of the generator.

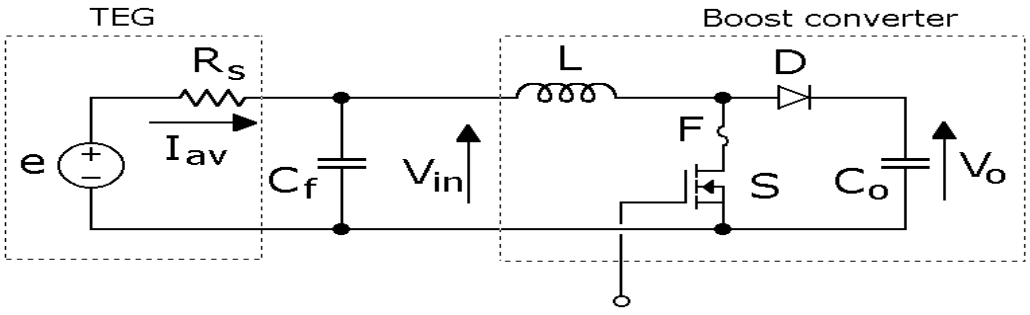

Fig. 2 *Boost converter used for maximum power tracking*

The Boost converter of Fig.2 may be designed to operate in either Discontinuous or Continuous Inductor Current Mode (DICM/CICM) can be used. It would initially appear that there is no possibility for CICM due to the possible absence of a load - it could happen so that the thermal source provides power at times when there is no load (R_L in Fig.1) connected to the system, so the converter only charges the storage capacitor. However, it should be considered that the storage capacitor, C_o in Fig.2, will typically be in the order of tens or hundreds of Farads, resembling a stiff DC voltage source. An effective load resistance can then be defined as follows.

The output power of the converter is:

$$P_o = V_o I_{C_{AVG}} \quad (1)$$

Where, I_{CAVG} is the average capacitor charging current.

And the input power (while in MPT mode):

$$P_{in} = \frac{V_{in}^{\ 2}}{R_s} \tag{2}$$

By equating the input and output power:

$$I_{C_{AVG}} = \frac{V_{in}^{\ 2}}{V_o R_s} \tag{3}$$

An effective load resistance can now be defined:

$$R_e = \frac{V_o}{I_{C_{AVG}}} = R_s \frac{V_o^{\ 2}}{V_{in}^{\ 2}} \tag{4}$$

It then applies, as generally known, that the converter operates in the DICM when (5) is satisfied.

$$k < \frac{t_{on}}{T}\left(1 - \frac{t_{on}}{T}\right)^2 \tag{5}$$

$$\text{Where,} \qquad k = \frac{2Lf}{R_e} \tag{6}$$

And t_{on} is the time during which switch S is in the ON state, and f=1/T is the switching frequency.

If (5) is not satisfied then the converter indeed operates in the CICM.

It should be mentioned that in deriving the MPT-related equations, the source voltage, e, may not be used, as it is not easily measurable in practice. Apart from causing a momentary open circuit [3], with its associated disadvantages, the only way to measure this voltage is by employing an auxiliary TEG cell with no load across it, placed close to the main TEG cells. However, this arrangement cannot guarantee correct measurement in the case of non-even thermal distribution across all the cells, and also increases the cost/complexity of the system.

A1. DICM

In order to analyse the MPT operation of the converter under any mode, the equivalent input resistance of the converter must be known. Equating this resistance with the internal source (TEG) resistance will then yield the necessary control function.

The equivalent input resistance of the converter in DICM can be based on the average inductor current. From Fig.2 and Fig.3, equations (7) and (8) can be derived.

$$\hat{I} = \frac{V_{in}}{L} t_{on} \tag{7}$$

$$\hat{I} = \frac{V_o - V_{in}}{L} \delta \tag{8}$$

The average inductor current can then be found from (9).

$$I_{av} = \frac{1}{T}\frac{1}{2}\hat{I}(t_{on} + \delta) \xrightarrow{(7)\&(8)} I_{av} = \frac{V_{in} t_{on}^{\ 2} V_o}{2LT(V_o - V_{in})} \tag{9}$$

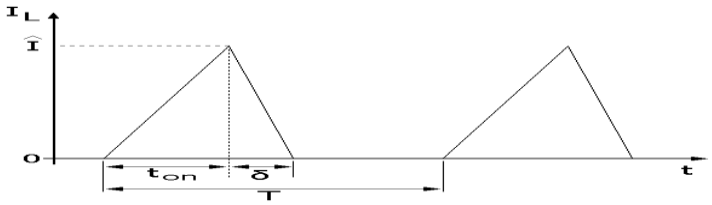

Fig. 3 *Boost inductor current in DICM*

The equivalent input resistance of the converter can then be defined as:

$$R_{in} = \frac{V_{in}}{I_{av}} = \frac{2L(V_o - V_{in})}{t_{on}^2 V_o f} \tag{10}$$

For maximum power transfer, it applies that $R_{in}=R_s$. The required switch turn-on time can then be found by rearranging (10) to:

$$t_{on} = \sqrt{\frac{2L(V_o - V_{in})}{V_o f R_s}} \tag{11}$$

This equation indicates that MPT control can be achieved only by knowledge of the input/output voltages. Both PWM and PFM can be used to implement this function.

A2. CICM

In CICM, it is known that the average inductor current of a Boost converter is:

$$I_{av} = \frac{I_o}{\left(1 - \frac{t_{on}}{T}\right)} \tag{12}$$

and the input voltage relates to the other variables as follows:

$$V_{in} = V_o\left(1 - \frac{t_{on}}{T}\right) \tag{13}$$

The equivalent input resistance of the converter can then be defined as:

$$R_{in} = \frac{V_{in}}{I_{av}} = \frac{V_o\left(1 - \frac{t_{on}}{T}\right)^2}{I_o} \tag{14}$$

Substituting I_o in (14) (using equations related to power equilibrium) always cancels the term R_{in} and results in equation (13). This means that R_{in} cannot be defined in terms of the input and output voltages. The output current (or the input current if (14) is rearranged) is required for MPT control.

B. Uncontrolled converter operation

It is possible to allow the converter to operate with a fixed duty ratio and accept any deviation from the maximum power transfer due to changes in the source or storage capacitor voltage, e and V_o respectively in Fig.2. An evaluation of the expected deviation in power transfer is presented below, for both DICM and CICM, in order to assess what is the control effort otherwise required to maintain MPT – a criterion that relates to the difficulty of designing a control system in either case.

Referring to Fig.2, the power drawn by the Boost converter (not under MPT but generally) is:

$$P = I_{av} e - I_{av}^2 R_s \tag{15}$$

The average input current of the converter in DICM as a function of the source and output voltage is:

$$I_{av} = \frac{-2Lf(V_o - e) - R_s D^2 V_o \pm \sqrt{\Delta}}{4LfR_s} \tag{16}$$

where $\Delta = 4L^2 f^2 (V_o - e)^2 + R_s^2 D^4 V_o^2 + 4Lf(V_o - e)R_s D^2 V_o - 8LfR_s e D^2 V_o$

The maximum power that can be drawn by the converter is:

$$P_m = \frac{e^2}{4R_s} \tag{17}$$

Fig.4a shows the plot of the ratio of equations (1) and (4). It reveals how different the power transfer is from the maximum one if the converter works with constant duty ratio as the input and output voltages vary. The duty ratio has been fixed to a value that evenly distributes the curvature around the surface. The plot is unaffected by the value of R_s, L

and *f* as long as discontinuous operation is considered. It is shown that the maximum deviation in power is around 12%. This loss can be avoided if a variable duty ratio/frequency control scheme is implemented so as to keep the converter at maximum power transfer.

Using similar methods, the plot of Fig.4a was generated for CICM, shown in Fig.4b. The plot was generated for a duty ratio that gives the smallest deviations in power. Yet, it is obvious that these deviations are quite large, especially at low source voltages. This is an indication that the CICM sets higher requirements on the MPT control than DICM does.

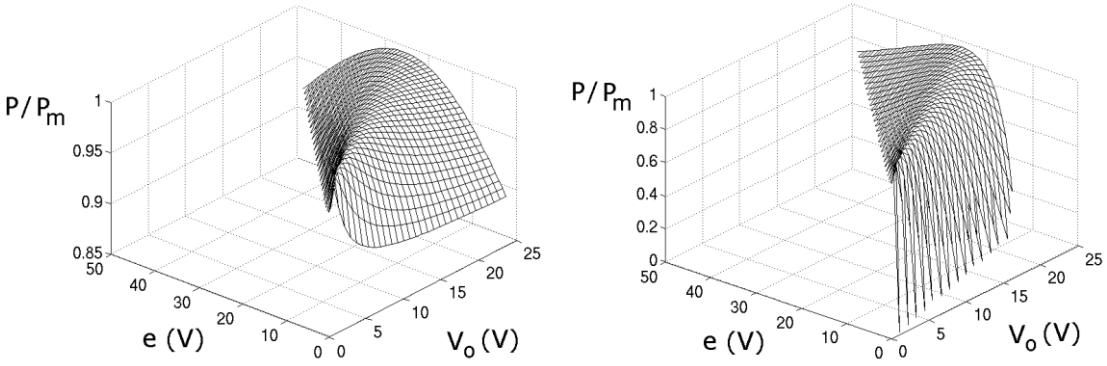

(a) (b)

Fig. 4. *Operation with fixed duty ratio. (a) DICM, (b) CICM.*

Taking into account all the above considerations, the DICM is found to be more suitable for the application. It requires smaller control efforts to keep the converter in MPT and it does not require the use of a current sensor. Apart from these, it will be shown next that it is possible to operate the converter on the boundary of DICM, where certain advantages come into effect.

C. PFM vs. PWM

Having concluded that operation in the DICM is preferable, the control method must be investigated. PWM is widely known, however, there is also the PFM method, where the on-time of the converter switch is fixed and the frequency is variable. To express all the equations described above in terms of PFM control, it is sufficient to replace the duty ratio notation with equation (18).

$$D = t_{on} f \tag{18}$$

The main difference between the two control methods lies in their capability to keep the converter in the DICM. It will be shown that the PWM method requires very small inductance values to maintain the DICM. Small inductance values however result in higher inductor and switch currents and therefore reduced efficiency.

The evaluation is based on the value of inductance required for each method to maintain operation on the boundary between DICM and CICM. That is, when (19) is satisfied:

$$k = D(1-D)^2 \tag{19}$$

For PWM, *D* is found by (11) and *k* is found from considering (4) and (6), equation (20).

$$k = \frac{2LfV_{in}^{\ 2}}{R_s V_o^{\ 2}} \tag{20}$$

The solution to (20) is then:

$$L = \frac{R_s V_o \left(V_o^{\ 2} - V_o V_{in} - V_{in}^{\ 2}\right)}{2f\left(V_o - V_{in}\right)\left(V_o^{\ 2} - V_o V_{in} + \sqrt{V_o\left(V_o V_{in}^{\ 2} - V_{in}^{\ 3}\right)}\right)} \tag{21}$$

This means that for PWM, in order to maintain DICM, the inductance must always fall below the value indicated by (21).

To find the minimum value of L for the whole range of operation, one needs to consider the maximum input voltage and minimum output voltage. This will be shown later in Fig.5, as a comparison with PFM control.

For PFM, using the t_{on} notation, equation (18), the control function, equation (11), turns into (22) (variable frequency).

$$f = \frac{2L(V_o - V_{in})}{V_o R_s t_{on}^{\ 2}} \tag{22}$$

Substituting (22) to (20) we obtain k in terms of t_{on}:

$$k = \frac{4L^2 V_{in}^{\ 2}(V_o - V_{in})}{V_o^{\ 3} R_s^{\ 2} t_{on}^{\ 2}} \tag{23}$$

Also, in (19), the duty ratio is replaced with:

$$D = f t_{on} = \frac{2L(V_o - V_{in})}{V_o R_s t_{on}} \tag{24}$$

The solution to (19), considering (23) and (24) is then:

$$L = \frac{1}{2} R_s t_{on} \tag{25}$$

An interesting point is revealed by (25). It shows that the solution to (19) is independent of the input/output voltages when PFM control is used. If the inductance has the value indicated by (25), then the converter operates on the boundary between DICM and CICM under all conditions.

That fact that the converter operates with varying frequency is typically considered as a disadvantage, due to the effect of this on the design/size of the filtering components. However, in this case, a super capacitor is used at the output of the converter, rendering the output filter sufficiently large even for very low frequencies. The remaining problem is the input filtering component, C_f in Fig.2, which should be large enough to effectively perform filtering at the minimum operating frequency. However, this proves to be not particularly problematic due to two reasons. The first reason is that the typically low output voltage of TEG cells translates to a low voltage rating for the filtering capacitor, leading to reduced size. The second and more important reason is that the converter spends very little time operating at the minimum frequency, and so a relaxation may be applied in the selection of C_f, i.e. a lower value/size may be allowed. The reason for which the converter spends very little time operating at the minimum frequency is the following: first one shall consider that the minimum operating frequency occurs when the output voltage is close to the input voltage, Eq.(28), that is when the super capacitor is almost discharged and the TEG voltage is at its maximum – that is when these two voltages become comparable. This is the case where the TEG is supplying the highest output power and the super capacitor is at its lowest charge state, in which case the rate of charging of the super capacitor is faster than under any other condition - taking into account $E=0.5CV^2$, for the same amount of power sent to the capacitor its voltage rises faster when the latter is discharged.

Fig.5 shows the relation between the inductance needed in PWM and PFM for operation on the boundary of DICM/CICM. The plot applies for any value of R_s; also, in order to make the comparison, it has been assumed that the turn on time of the switch in PFM is equal to the period of switching in PWM ($t_{on}=1/f$). For large voltage conversion ratios, the inductance needed in both cases is almost the same. However, when nominal input voltage (around 5 V in this case) and low output voltage is considered, PWM requires much smaller inductance in order to keep the converter in DICM. The reason for this is that the effective resistance of the load under MPT is dependent on the input/output voltages, equation (4). With low output voltage and nominal input voltage, the effective load resistance becomes very low, forcing the operation to DICM. With PFM control this situation can be overcome by variation of the switching frequency. In fact the compensation is acting complementary to the effect, resulting in guaranteed operation on the boundary of DICM, when (25) is satisfied.

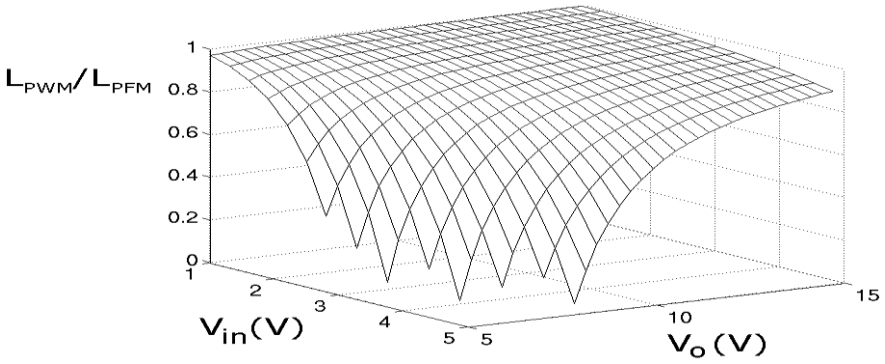

Fig. 5. *Comparison of inductance needed for boundary DICM MPT operation, between PWM and PFM.*

The operation of the converter on the boundary of DICM is advantageous. Of all the operating points in DICM this is the one with the lowest peak-to-average inductor current. Also, the Boost diode self-commutates off because its current goes to zero before the switch turns on. In its turn, the switch operates with Zero Current Switching, which means that its turn-on losses are greatly reduced. Finally, the realisation of synchronous Boost converter scheme is quite easier in this mode, since the switching times for the devices are easily defined. These advantages are further pronounced due to the fact that the operation on the boundary of DICM is achieved for the whole range of input/output voltage conditions.

III. DIGITAL CONTROLLER

The control function for the operation of the converter in MPT is given by (22). The input and output voltages must be fed back to the controller. The controller then will force the system to settle in MPT. Analogue electronics can be used to implement the control function. However, as explained in the introduction, the MPT system might have to experience wide temperature variations if used in TEG applications. In order to avoid the DC offsets and thermal drifts associated with analogue electronics and increase the accuracy of the MPT converter, it is suggested to make use of a digital controller.

Using a DSP to implement (22) would be unreasonable and characterised as underutilisation of the processor, even with the simplest cores. Low-end microcontrollers, on the other hand, would lack the required resources to implement the control function in real time. Medium power microcontrollers would be more suitable for the application.

However, it is possible to lower the cost of the system by using a low-end microcontroller along with a Look Up Table, as shown in Fig.6. The LUT can directly indicate the required switching frequency, based on the sampling of V_{in} and V_o, and then the microcontroller can generate the frequency with a minimum number of calculations. This arrangement poses minimum overhead to the microprocessor, allowing it to perform other background tasks that might be useful to neighbouring systems.

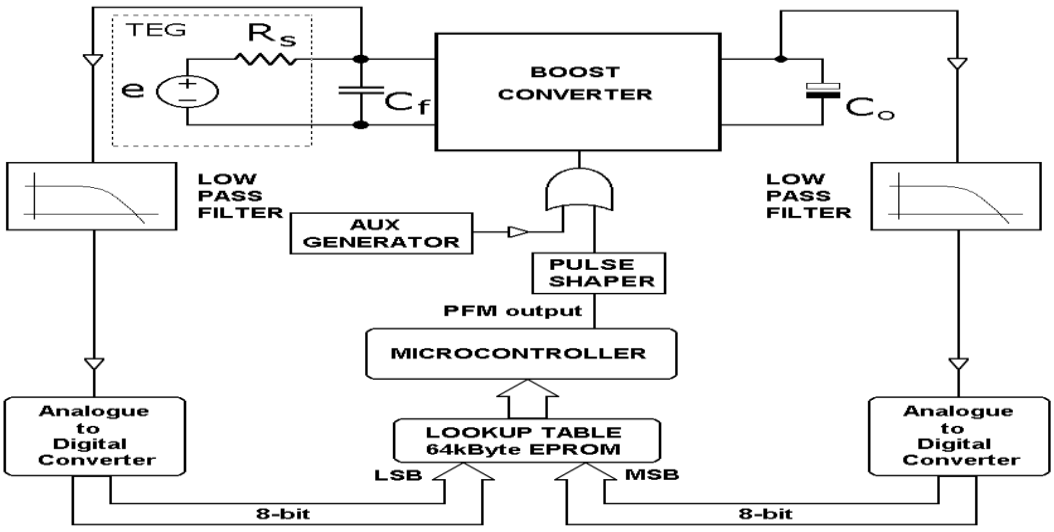

Fig. 6. *Microcontroller based MPT system.*

The LUT can be implemented with an EPROM. The irregularity of the above system is that the control function leads to a two-dimensional LUT. This issue can be overcome by breaking the linear input address of an EPROM into two blocks, Fig.7. For a standard 8-bit system, a 16-bit input EPROM is needed, specifically the 27C512. The programming of the memory is based on (22) and (26).

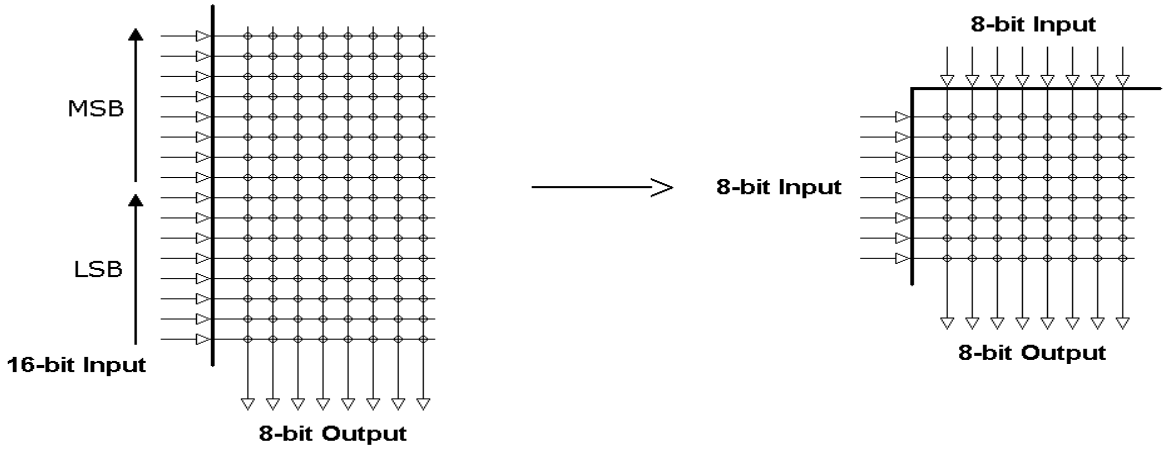

Fig.7. *'Folding' the linear address of a 27C512 EPROM to form a 2-D LUT.*

The output of the LUT is converted to a switching frequency signal by the microcontroller. The relation frequency=*f*(LUT) is not linear in most cases due to microcontroller computation delays. These must be taken into account when programming the EPROM. For example, with the microcontroller used for the experiment, there was a fixed computational delay of 1.4μs and a further 0.4μs was added for each of the 256 states of the output of the LUT. Therefore, the PFM output (Fig.6) frequency as a function of the LUT value can be calculated by (26).

$$f(MHz)=\frac{1}{1.4+0.4(256-LUT)} \tag{26}$$

Two extra functions can be implemented in the LUT. The first is storage capacitor overvoltage protection, by programming for zero LUT output when V_o is above a defined limit. The second function embedded into the LUT is the shutdown of the converter when $V_{in}>V_o$; again zero output is generated. According to (26), zero value from the LUT will result to low frequency operation. However, a separate logic, hardware or software based, can detect the zero output of the LUT and disable the switch driver.

The output of the microcontroller is a short pulse at the required frequency. A specific value for the t_{on} of the switch is also required by design. This is performed by a pulse shaper, Fig.6, which when triggered by the PFM output produces a pulse of fixed duration.

It is shown in Fig.6 that the control signal is either fed from the microcontroller or an auxiliary generator. The purpose of this generator is to aid the start-up of the converter. In the initial state of operation, the storage capacitor is charged through the Boost diode, as its voltage is lower than the source voltage. Due to this clamped operation, the MPT system cannot be initiated as it sees zero voltage difference between input and output; equation (22) then outputs a zero switching frequency. The generator produces bursts of pulses at frequent intervals in order to test whether the converter is ready to operate in MPT, that is, when the storage capacitor voltage reaches half the source voltage. The frequency of these bursts is not critical, but should not be very high so as to avoid interference with the initial charging of the capacitor; a frequency of 200Hz was selected for the prototype. The auxiliary generator is seen in Fig.6 as an external to the microcontroller system. However, this is shown for clarity, as this function can also be microcontroller embedded.

IV. CONVERTER DESIGN & EXPERIMENTAL RESULTS

A. Design

The design of the converter is straightforward and begins with the selection of input and output voltage ranges. These will determine the maximum and minimum frequency of operation:

$$f_{MAX} = \frac{2L\left(V_{oMAX} - V_{inMIN}\right)}{V_{oMAX} R_s t_{on}^{\ 2}} \tag{27}$$

$$f_{MIN} = \frac{2L\left(V_{oMIN} - V_{inMAX}\right)}{V_{oMIN} R_s t_{on}^{\ 2}} \tag{28}$$

A value for t_{on} can be given to set the two frequencies to reasonable levels. It should be considered, however, that the turn-on time can never exceed the minimum period of switching, equation (29).

$$t_{on} < \frac{1}{f_{MAX}} \tag{29}$$

The value for the Boost inductance can then be calculated by the boundary DICM constraint:

$$L = \frac{1}{2} R_s t_{on} \tag{30}$$

The maximum peak inductor (equal to maximum switch current) can be calculated by (31).

$$\hat{I}_{MAX} = \frac{V_{inMAX}}{L} t_{on} \tag{31}$$

An iterative design method can be used with (27)-(31) if a specific result is required, for instance maximum peak current below a predefined limit.

B. Experiment

A prototype was built to validate the theoretical findings, as shown in Fig.2. The values of the components used are listed in Table I. The prototype was built for a TEG installation with an open circuit voltage between 4-10 V, therefore, under MPT, a converter input voltage of 2-5 V. The output voltage range was 7-15 V; taking into account $E=0.5CV^2$, this means that the capacitor utilisation is just above 78%.

TABLE I
PROTOTYPE COMPONENT VALUES - Circuit of Fig.2

L	5 μH
R_s	1 Ω
C_o	1 F
C_f	1000 μF
D	BYV42
S	IRFZ44

The peak inductor current was chosen to be just twice the maximum average current (5 A), so an inductance value of 5μH and a t_{on} of 10 μs were chosen, equations (30) & (31). According to the above, (27) and (28) give f_{min}=29 kHz and f_{max}=93 kHz.

In order to test the circuit, the internal voltage of the TEG had to be measured. Therefore, a power supply with an externally connected resistor was used instead. The power supply was internally compensated so it did not present any apparent internal resistance in addition to the external one.

Fig.8 shows the converter waveforms for two operating conditions (V_o=7 V/f=71 kHz, V_o=14 V/f=86 kHz). It is shown that the input voltage of the converter has settled to half the source voltage, meaning that MPT is achieved. Equally important, and as theoretically predicted, it is shown that the inductor current remains on the boundary of discontinuity under these two different conditions.

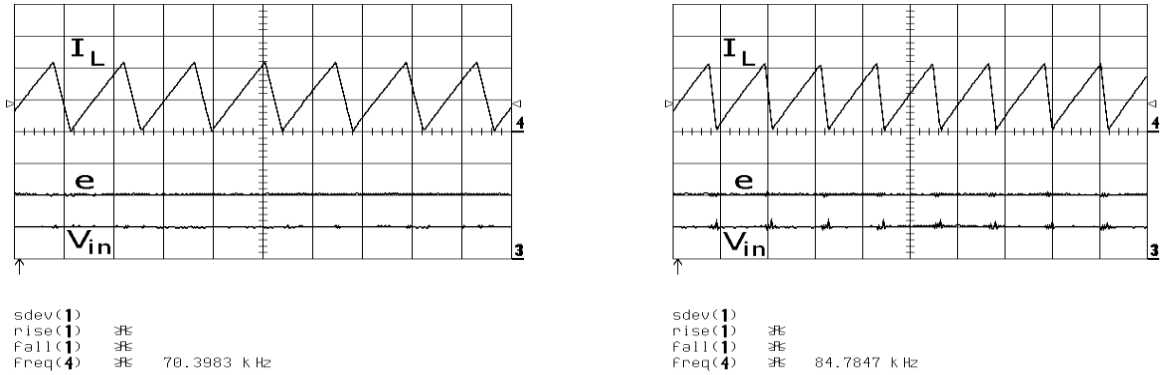

(a) (b)

Fig. 8. *DICM is maintained under different conditions. (a) V_o=7.5V (b)V_o=14.5V. Scales: I_L 2A/div, e 2V/div, V_{in} 2V/div, t 10μs/div, frequency shown in figure.*

Fig.9 shows the converter waveforms under nominal power (25 W) and an output voltage of 14.5 V (corresponding to f=66 kHz). The inductor current remains on the boundary of discontinuity and MPT is also retained. The peak inductor current is 10 A, twice the average input current. The voltage across the device appears to slide smoothly from V_o to zero with no apparent evidence of significant turn-on losses.

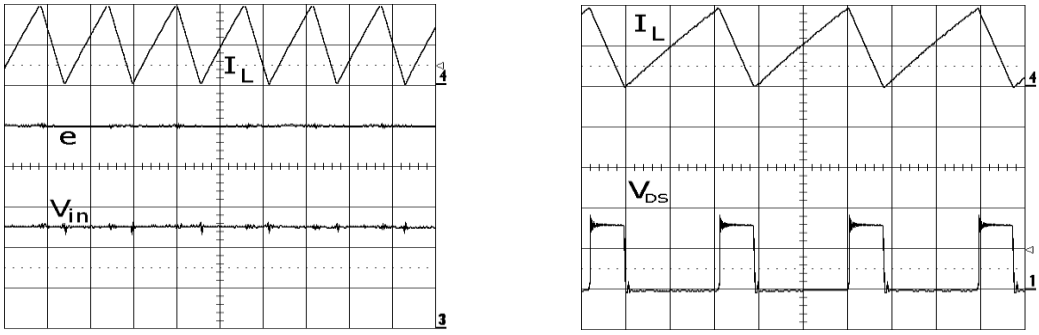

(a) (b)

Fig. 9. *Operation at nominal power. (a) Source/converter input voltages (b) voltage across converter switch. Scales: I_L 5A/div, e 2V/div, V_{in} 2V/div, t (a) 10μs/div (b) 5μs/div.*

The transient behaviour of the system is shown in Fig.10a. A time of around 10 ms is required for the system to settle after a step change of the source voltage from zero to 8V. This includes the time taken for the filter capacitor, C_f, to charge from R_s to 4V. For a thermal system, this dynamic response is sufficient in most cases. Fig.10b shows an arbitrary change of the source voltage, with the converter input voltage following closely at half the source voltage, indicating the precise tracking of the maximum power.

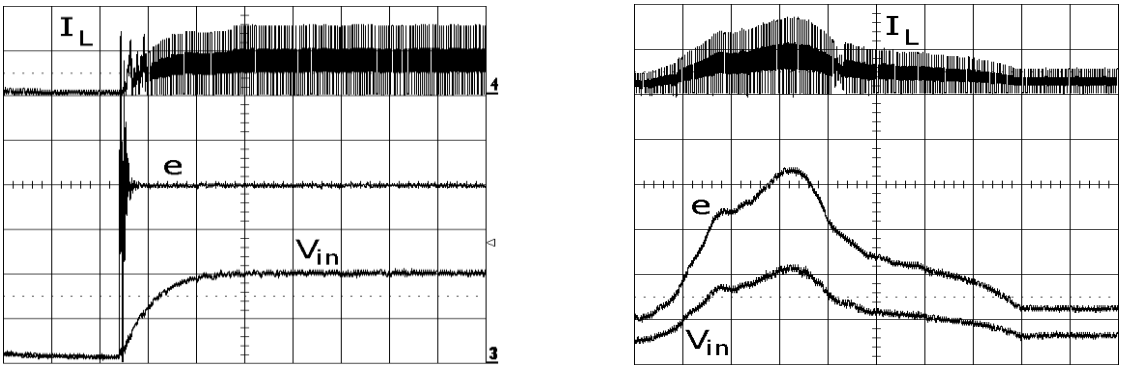

(a) (b)

Fig.10. *Transient behaviour of the MPT system. (a) Zero source voltage to 10V (b) arbitrary source voltage change. Scales: I_L 5A/div, e 2V/div, V_{in} 2V/div, t (a) 5ms/div (b) 0.5s/div.*

V. CONCLUSION

A maximum power tracking Boost converter has been described for use in supercapacitor energy storage from thermoelectric generators and other similar sources. The analysis of the converter has shown that the Discontinuous Inductor Current Mode operation is the most suitable for this application, also allowing the system to be current-sensorless. Furthermore it was shown that it is possible, with the use of the PFM control method, to establish operation on the boundary of the DICM throughout the whole range of input/output voltage and while maintaining maximum power tracking control. This operation results in the lowest possible converter losses, both conduction and switching. A simple, low-cost digital controller with a low-end microcontroller and a Look-Up-Table was described for the control of the converter. Measurements from a 25W prototype have verified the capability of the converter to operate on the boundary of DICM under any condition and the accuracy of the digital controller in extracting maximum power from the source.

REFERENCES

[1] Jorge Vázquez, Miguel A. Sanz-Bobi, Rafael Palacios, Antonio Arenas, "State of the Art of Thermoelectric Generators Based on Heat Recovered from the Exhaust Gases of Automobiles", Proceedings of the 7th European Workshop on Thermoelectrics, Paper #17, Oct 2002, Pamplona, Spain.

[2] Kushch, A.S.; Bass, J.C.; Ghamaty, S.; Eisner, N.B., "Thermoelectric development at Hi-Z technology," *Proceedings International Conference on Thermoelectrics*, pp.422,430, 2001.

[3] Laird, I.; Lu, D. D –C, "High Step-Up DC/DC Topology and MPPT Algorithm for Use With a Thermoelectric Generator," *Power Electronics, IEEE Transactions on* , vol.28, no.7, pp.3147,3157, July 2013.

[4] Jungmoon Kim; Chulwoo Kim, "A DC–DC Boost Converter With Variation-Tolerant MPPT Technique and Efficient ZCS Circuit for Thermoelectric Energy Harvesting Applications," *Power Electronics, IEEE Transactions on* , vol.28, no.8, pp.3827,3833, Aug. 2013.

[5] Rae-young Kim; Jih-Sheng Lai, "A Seamless Mode Transfer Maximum Power Point Tracking Controller For Thermoelectric Generator Applications," *Power Electronics, IEEE Transactions on* , vol.23, no.5, pp.2310,2318, Sept. 2008.

[6] J. Damaschke, "Design of a low-input-voltage converter for thermoelectric generator," *IEEE Trans. Ind. Appl.*, vol. 33, no. 5, pp. 1203–1207, Sep./Oct. 1997.

[7] Hidaka, A.; Tsuji, T.; Matsumoto, S., "A thermoelectric power generation system with ultra low input voltage boost converter with maximum power point tracking," *Renewable Energy Research and Applications (ICRERA), 2012 International Conference on* , vol., no., pp.1,5, 11-14 Nov. 2012.

[8] Damaschke, J.M., "Design of a low-input-voltage converter for thermoelectric generator," *Industry Applications, IEEE Transactions on* , vol.33, no.5, pp.1203,1207, Sep/Oct 1997-doi: 10.1109/28.633797

[9] Roshan, Y.M.; Moallem, M., "Maximum power point tracking using boost converter input resistance control," *Industrial Electronics (ISIE), 2012 IEEE International Symposium on* , vol., no., pp.1795,1800, 28-31 May 2012

[10] T. Esram and P. Chapman, "Comparison of photovoltaic array maximum power point tracking techniques," *IEEE Trans. Energy Convers.*, vol. 22, no. 2, pp. 439–449, Jun. 2007.

[11] I. Laird, H. Lovatt, N. Savvides, D. Lu, and V. Agelidis, "Comparative study of maximum power point tracking algorithms for thermoelectric generators," in *Proc. Power Eng. Conf. Australasian Univ.*, Dec. 2008, pp. 1–6.

[12] E. J. Carlson, K. Strunz, and B. P. Otis, "A 20 mV input boost converter with efficient digital control for thermoelectric energy harvesting," *IEEE J. Solid-State Circuits*, vol. 45, no. 4, pp. 741–750, Apr. 2010.

[13] Y. K. Ramadass and A. P. Chandrakasan, "A batteryless thermoelectric energy-harvesting interface circuit with 35 mV startup voltage," *IEEE J. Solid-State Circuits*, vol. 46, no. 1, pp. 333–341, Jan. 2011.

[14] Rafael Palacios, Ming Zhu Li, "Electrical Properties of Commercial Thermoelectric Modules", Fourth European Workshop on Thermoelectrics, pp. 159-162, September 1998, Madrid, Spain.

[15] J.J. Kiely, D.V. Morgan, D.M. Rowe, J.M. Humphrey, "Low cost miniature thermoelectric generator", Electronics Letters, Vol. 27, Issue 25, pp.2332-2334, 5 Dec. 1991.